Journal of Anatomy

J. Anat. (2016) **229**, pp422–435 doi: 10.1111/joa.12487

Shape variation and ontogeny of the ruminant bony labyrinth, an example in Tragulidae

Bastien Mennecart and Loïc Costeur

Naturhistorisches Museum Basel, Augustinergasse 2, 4001 Basel, Switzerland

Abstract

Despite its growing use in anatomical and ecological studies, the morphological variability and ontogenetic development of the bony labyrinth have very rarely been investigated in ruminants. Here we study its morphology in 15 adult and 10 juvenile specimens in the three extant tragulid ruminant genera. Intraspecific and interspecific variability is quantified using morphometric and 3D geometric morphometrics analyses. The bony labyrinth of *Tragulus*, *Hyemoschus*, and *Moschiola* is strikingly different, clustering in clearly different morphospaces despite similar ecological adaptations. Although the bony labyrinths within two species of the same genus cannot be distinguished from each other based on the chosen semi-landmarks, discrete interspecific differences exist. We were able to show for the first time that an artiodactyl mammal in a late fetal stage possesses an almost fully formed bony labyrinth similar to that of adults. No significant change either occurs in size or morphology after ossification of the petrosal bone. Some intraspecific variation is observed on the shape of the lateral semi-circular canal, the size and shape of the common crus, the coil of the cochlea or the stapedial ratio. Variable structures are expected to be highly informative characters for a large cladistic analysis. They can be used for phylogenetic studies in ruminants. Incorporating juvenile specimens in studies is not problematic, as they fall within the morphological range of adults.

Key words: artiodactyla; fetus; geometric morphometrics; inner ear region; morphology; petrosal bone.

Introduction

The morphology of the bony labyrinth and inner ear has been shown to provide valuable information about phylogeny, development, and functional adaptations in several mammal groups (e.g. primates: Spoor et al. 2007; David et al. 2010; Lebrun et al. 2010; Gunz et al. 2012; carnivores: Grohe et al. 2015; rodents: Schwarz, 2012; marsupials: Sánchez-Villagra & Schmelzle, 2007; Schmelzle et al. 2007; Alloing-Séguier et al. 2013; bats: Davies et al. 2013; xenarthrans: Billet et al. 2012, 2015). Until recently, it was difficult to study the ear region of the skull without partially destroying it. This is the main reason why few comparative works and very few attempts at looking at character variability or ontogenetic changes in mammals have been carried out. These studies nonetheless represent a prerequisite when one tries to understand the evolution and development of an anatomical structure. With the use of non-destructive computed tomography-based methods, several of the most recent works cited above have sampled large amounts of species to focus on phylogenetically relevant anatomical differences between large clades of mammals (e.g. Ekdale, 2013). However, developmental changes and intraspecific variability were rarely included in these works. When ontogeny was investigated, it indicated that intraspecific post-natal ontogenetic changes are different depending on the group under study (e.g. Jeffery & Spoor, 2004; Sánchez-Villagra & Schmelzle, 2007). Except for histological studies (Van Arsdel & Hilleman, 1951; Solntseva, 2010; Maier, 2013) and works on humans (Jeffery & Spoor, 2004; Toyoda et al. 2015), no pre-natal stage (fetus) has ever ever included in a study on the non-human mammalian bony labyrinth. A study on human fetuses (Jeffery & Spoor, 2004) indicated that the bony labyrinth undergoes few changes after ossification, which is achieved before birth. Conversely, changes are higher in the development of some marsupials because ossification is achieved later, after birth (Sánchez-Villagra & Schmelzle, 2007). A pilot work on an ontogenetic series of the grey short-tailed opossum *Monodelphis domestica* (Ekdale, 2010) confirmed that not much change occurred after ossification. Ruminants achieve ossification of the petrosal bone before birth (see Maier, 2013) and thus few changes in the morphology and shape of the bony labyrinth are expected to occur after birth.

Correspondence
Bastien Mennecart, Naturhistorisches Museum Basel, Augustinergasse 2, 4001 Basel, Switzerland. E: mennecartbastien@gmail.com

Accepted for publication *30 March 2016*
Article published online *1 June 2016*

Large intraspecific morphological variation seems to occur only in special cases, as in the three-toed sloth, where a release of selective pressure on semi-circular canals controlled by the animals reduced activity pattern, or slow motion, leading to a high amount of variation (Billet et al. 2012). The same study showed no such variation in a range of faster-moving placentals. Most ruminants are comparatively fast-moving animals for which little morphological variation can be expected. If we exclude studies on the human ear, some marsupials (Sánchez-Villagra & Schmelzle, 2007; Schmelzle et al. 2007; Ekdale, 2010), some primates (Spoor & Zonneveld, 1995, 1998; Gunz et al. 2012), sciurid rodents (Pfaff et al. 2015) and the golden hamster (Van Arsdel & Hilleman, 1951), musteloid carnivores (Grohe et al. 2015), the horse (Danilo et al. 2015), and several xenarthrans (Billet et al. 2012, 2015), there have been few studies with a focus on intraspecific, interspecific or intra-familial morphological variability and they have mostly been based on post-natal ontogeny. The aims were as diverse as studying phylogeny, palaeoecology or ecology, palaeobiology, development or evolution.

Morphological variability and ontogeny of the bony labyrinth has never been investigated in ruminants. The only large descriptive works including ruminant bony labyrinths are more than 100 years old (Hyrtl, 1845; Gray, 1907, 1908). Only seven of the more than 200 extant species of ruminants were described in these studies from radiographs or bony labyrinth casts, which sometimes do not reflect the proper shape of this structure. Recent works based on histological slides (Maier, 2013) focus on the development of the entotympanic bone in late fetal stages. Another comparative work not directly related to ruminant issues describes the bony labyrinth of the tragulid *Moschiola* (Orliac et al. 2012). In addition, the bony labyrinths of fossil ruminants very rarely have been described and are only now beginning to be known (Costeur, 2014; Costeur et al. 2014; Mennecart & Costeur, in press). The ruminant fossil record is comparatively extensive. In light of the remaining issues pertaining to the evolutionary history of ruminants and of the potential of the ear region to provide phylogenetic characters, using the bony labyrinth could help resolve many problems at different hierarchical levels (e.g. origin of crown groups, clade divergence, status of stem pecorans, or debated phylogenetic positions, see Mennecart & Costeur, in press).

The Tragulidae are the basalmost family of extant ruminants comprising three living genera and eight recognized species (Wilson & Reeder, 2005). They are the only living non pecoran ruminants, hence their separation in a 'Tragulina' clade (Hassanin et al. 2012). Tragulidae are known in the fossil record from the Late Eocene of Asia (*Archaeotragulus*; see Métais et al. 2001) but remained extremely rare during the Palaeogene (Mennecart et al. 2011; Mennecart & Métais, 2015). They became quite abundant in the Neogene with such forms as *Dorcatherium* or *Afrotragulus* (Gentry et al. 1999; Rössner, 2007; Geraads, 2010; Sánchez et al. 2014). Living taxa are diminutive animals inhabiting dense tropical forest environments of equatorial Africa and South-East Asia (Meijaard & Groves, 2004; and for the ecology of *Hyemoschus* see Dubost, 1975). Tragulid bony labyrinths were published for comparison with *Diacodexis*, the oldest known artiodactyl (Orliac et al. 2012) and recently have been included in phylogenetic studies (Mennecart & Costeur, in press). Nevertheless, the intraspecific, interspecific or intrafamilial variability of the bony labyrinth has never been studied within closely related taxa inside the same ruminant family. This is the focus of this work.

In this study, using 3D geometric and classical morphometrics, we describe and analyse the morphological variation of the bony labyrinth of the lesser mouse deer *Tragulus kanchil*. Through the study of five ontogenetic stages (from fetal to adult stages), we give insights into the morphological variability of this structure inside a species. We have added the bony labyrinth of a closely related species, *Tragulus napu*, to this analysis to see whether interspecific disparity is higher than intraspecific variability. Moreover, we compare our *Tragulus* sample with the water chevrotain (*Hyemoschus aquaticus*) and with the sister taxon of *Tragulus*, the spotted chevrotain (*Moschiola meminna*), which are both monospecific genera (for tragulid phylogeny, see Sánchez et al. 2014 and Mennecart & Costeur, in press). Thus we cover all three living tragulid genera and are able to understand to what extent the bony labyrinth of tragulids reflects taxonomic affinities.

Materials and methods

Specimens

We have reconstructed the endocast of the bony labyrinth of six adult specimens, three different juvenile stages, and one fetus of the Tragulidae *Tragulus kanchil*, one adult *Tragulus napu*, three adult specimens and five juveniles at different stages of *Hyemoschus aquaticus*, and five adult specimens and one juvenile *Moschiola meminna* (see Table 1). All specimens come from the collection of the Natural History Museum Basel (NMB) and were mostly sampled in the late 19th or early 20th centuries (see Table 1 for more information). Subspecies of *T. kanchil* have been described mostly based on coat patterns and often show large craniometric overlap (Meijaard & Groves, 2004; Groves & Grubb, 2011). The studied specimens have not been attributed to subspecies but all come from geographic areas where *T. kanchil* is represented, often as the only tragulid species (Meijaard & Groves, 2004; Table 1). Ages of the sampled individuals are not precisely known as they were sampled in the wild more than 100 years ago. Methods to estimate the age of *Tragulus* and *Moschiola* are not known, but approximation can be achieved using charts and data for ruminants gathered in Hillson (1986) and Dubost et al. (2010) for the water Chevrotain *H. aquaticus*. All juvenile stages have deciduous upper premolars. The first one (NMB MAMM 1532) is a fully formed fetus. Gestation periods of 140–154 days are known in *Tragulus javanicus* and *T. napu*, respectively (Dubost et al. 2010). Considering the fully formed body of this fetus, the size of its head (40.5 mm), the presence of whiskers and cilia, we estimate it to be in a late fetal stage. The

Table 1 Data and measurements for the specimens used in this study.

Species	NMB accession number	Sex	Age	Laterality	Originating	Resolution (mm)	Skull size (mm)	Number of turns	Length of cochlea (mm)	Cochlear aspect ratio	Volume labyrinth (mm^3)	ASCH	ASCW	PSCH	PSCW	LSCL	LSCW	Stapedial ratio	Angle ASC-PSC	Angle ASC-LSC	Angle PSC-LSC	Centroid size
Tragulus kanchil	MAM 1532	?	Fetus	Left	Sumatra, ID	17.5	40.5	3.50	37.05	0.62	38.38	3.46	3.26	2.87	3.18	3.17	3.26	1.97	86.00	88.00	94.00	86.27
T. kanchil	C2988	M	Juvenile	Left	Sumatra, ID	25	59.1	3.75	37.82	0.62	38.12	3.45	3.23	2.89	3.04	3.03	3.14	1.73	92.00	85.00	84.50	83.09
T. kanchil	C2132	?	Juvenile	Left	Penang, My	25	77.1*	3.50	35.91	0.69	38.80	3.44	3.47	3.11	3.44	3.14	3.19	1.84	87.00	86.00	88.00	84.45
T. kanchil	C3806	F	Juvenile	Left	Sumatra, ID	25	90.67	3.75	36.57	0.68	36.35	3.79	3.50	3.27	3.48	3.20	3.34	1.98	87.50	85.00	87.00	83.28
T. kanchil	C3735	F	Adult	Left	Unknown	30	95.07	3.75	37.05	0.70	31.90	3.45	3.26	2.87	3.02	2.68	3.07	1.90	82.00	77.00	92.00	80.58
T. kanchil	C3791	M	Adult	Right	Sumatra, ID	20	91.68	3.75	39.15	0.63	37.90	3.64	3.40	3.10	3.29	2.88	2.94	1.66	83.00	86.00	94.00	84.78
T. kanchil	C3795	M	Adult	Leff	Sumatra, ID	25	89.69	3.75	36.67	0.68	31.80	3.69	3.34	3.30	3.41	3.16	3.17	1.76	84.50	84.00	93.50	80.31
T. kanchil	C3797	F	Adult	Left	Sumatra, ID	20	85.79*	4.00	36.54	0.63	35.74	3.46	3.39	3.19	3.34	3.04	3.47	1.65	89.00	86.00	93.00	82.28
T. kanchil	C3802	F	Adult	Left	Sumatra, ID	30	84.25*	3.50	34.77	0.65	35.76	3.16	2.84	2.85	2.64	2.86	3.13	1.81	85.50	81.00	90.00	81.61
T. kanchil	C1891	F	Adult	Right	Sumatra, ID	40	95.1	3.75	36.70	0.59	36.49	3.75	3.66	3.43	3.52	3.05	3.27	1.71	86.80	85.00	102.00	85.10
T. napu	10085	F	Adult	Lett	Borneo, ID	19.9	103.5	3.25	37.66	0.60	37.30	3.85	3.34	3.40	3.44	3.21	3.21	1.56	88.50	81.50	93.00	87.98
Moschiola meminna	C2589	M?	Juvenile	Lett	Sri Lanka	40	93.1	3.00	31.24	0.69	41.90	4.12	3.55	3.24	3.80	3.42	3.47	1.28	90.00	71.00	109.00	86.57
M. meminna	C2453	F	Adult	Lett	Sri Lanka	40	100.5	3.00	33.21	0.62	37.10	3.72	3.43	2.87	2.17	2.67	2.70	1.37	98.00	96.00	105.00	82.20
M. meminna	C1429	M	Adult	Lett	Sri Lanka	40	93.2*	3.00	32.49	0.59	42.60	4.23	4.14	3.26	3.74	3.02	3.37	1.41	84.00	73.00	100.80	89.71
M. meminna	C2319	F?	Adult	Lett	Sri Lanka	40	87.7	3.25	32.28	0.69	36.80	4.10	3.54	2.91	3.58	2.70	2.81	1.31	97.00	80.40	95.00	84.17
M. meminna	C1366	M	Adult	Lett	Sri Lanka	40	92.4	2.75	29.62	0.58	34.60	3.88	3.52	3.20	3.90	2.91	3.12	1.44	86.50	89.40	101.50	85.16
M. meminna	C2588	M	Adult	Lett	Sri Lanka	40	93.4*	3.00	32.57	0.68	46.60	4.51	4.16	3.72	4.01	3.03	2.86	1.51	97.00	75.00	102.00	93.72
Hyemoschus aquaticus	C1930	F	Juvenile	Right	SL	40	114.3	3.00	37.21	0.62	65.10	4.86	4.87	4.44	5.20	3.93	4.29	1.54	89.00	85.00	95.00	103.59
H. aquaticus	L11945	?	Juvenile	Right	Tchibati, CD	40	111.7	2.75	35.51	0.75	64.30	5.04	5.01	4.07	5.37	3.91	4.41	1.60	82.00	86.20	96.40	104.21
H. aquaticus	Lxx23	?	Juvenile	Lett	Kivu, CD	40	93.9	3.25	39.44	0.65	64.80	4.56	4.47	4.11	4.83	3.92	3.64	1.58	91.00	83.60	91.00	102.57
H. aquaticus	C2985	F	Juvenile	Right	Unknown	40	115*	3.00	38.24	0.65	70.10	5.15	4.85	4.38	4.94	4.07	4.15	1.51	90.70	80.80	91.40	109.08
H. aquaticus	C2499	M	Juvenile	Lett	SL	40	123.5*	3.00	36.41	0.64	61.00	4.99	4.53	4.40	5.21	4.12	4.14	1.51	84.50	79.80	88.30	105.90
H. aquaticus	L12132	F	Adult	Right	Kivu, CD	40	?	3.50	38.86	0.58	63.60	4.97	4.55	4.51	4.97	3.82	3.97	1.55	78.70	86.30	96.40	105.65
H. aquaticus	8699	M	Adult	Lett	Batouri, CM	40	138.1	3.00	39.76	0.62	68.70	4.65	4.60	3.96	4.80	3.36	3.99	1.70	89.00	79.80	86.40	103.68
H. aquaticus	C2692	F	Adult	Lett	Liberia	30	139.44	2.75	36.81	0.57	71.40	4.78	4.86	4.30	5.25	3.73	4.47	1.57	91.00	87.00	89.00	107.04

Cochlear length was measured by taking the increments along the most external curve of each turn and adding all increments. ASCH, height of anterior semi-circular canal; ASCW, width of anterior semi-circular canal; CC, common crus; LSCL, length of lateral semi-circular canal; LSCW, width of lateral semi-circular canal; PSCH, height of posterior semi-circular canal; PSCW, width of posterior semi-circular canal. CD, Democratic Republic of the Congo; CM, Cameroon; ID, Indonesia; SL, Republic of Sierra Leone. *Premaxillary bones broken, size underestimated.

approximate ages of the post-natal juveniles can be estimated at 2–4 months for NMB C2988 (first upper molar erupting, no second upper yet), at about 7 months to 1 year for NMB C2132 (first molar erupted, second upper molar erupting, no third molar), and at 1.5–2 years for NMB C3806 (third upper molar erupting, first and second upper molars fully erupted). No prenatal specimen of the other tragulids is included. Youngest specimens of *Hyemoschus* and *Moschiola* present an erupting M2, so are around a year old.

CT scanning

The specimens were scanned using high resolution X-ray computed tomography (Phoenix Nanotom®, GE at the Biomaterials Science Centre of the University of Basel, Switzerland). Scanning resolution varies between 17.5 and 40 μm (see Table 1). In all, 1440 equiangular radiographs were taken over 360° using an accelerating voltage of 90 kV and a beam current of 200 μA. Segmentation of the endocast of the bony labyrinths was done with AVIZO® 7.0 software (Visualization Sciences Group).

Measurements and nomenclature

Linear, angular, and volumetric measurements were made in the AVIZO® 7.0 software. Methodologies for measurements follow Ekdale (2013) and Macrini et al. (2013). The length of the cochlea was measured using AVIZO® 7.0 using the concatenation of *ca*. 100 segments. Nomenclature follows Orliac et al. (2012) and Macrini et al. 2013 (see Fig. 1).

Geometric mophometrics analyses

Left inner ears were preferably chosen. When left specimens were not available, the right one was reflected using the reflect application of LANDMARK EDITOR 3.6 software (Wiley, 2006). Digitalization of the specimens has also been performed using the LANDMARK EDITOR 3.6 software (Wiley, 2006). Seventy-seven curves were digitalized on the surface of the specimens (Fig. 2). For each curve, 10 equidistant semi-landmarks were then extracted from the curves. One additional landmark has been directly plotted on the surface of the specimens. The endolymphatic sac, even if phylogenetically informative (Mennecart & Costeur, in press) is not digitalized here due to the complexity of segmenting an open structure that can lead to inconsistencies. After several tests, we have decided not to integrate this structure in order to avoid an artificial Pinocchio effect for this area (von Cramon-Taubadel et al. 2007). A total of 686 landmarks were conserved to avoid superimpositions of several landmarks as well as artificial pressure in some areas. We have chosen a large number of semi-landmarks to characterize the shape of the bony labyrinth. We hypothesize that the number of semi-landmarks is proportional to the precision in taxonomical attribution (for different methods or taxonic precision see Gunz et al. 2012; Benoit et al. 2015; Billet et al. 2015; Grohe et al. 2015). Moreover, most of these methods use a skeletonized bony labyrinth, missing indications on the thickness of the structures that we wanted to analyse. Shape variation in the bony labyrinth morphology (disparity and similarity) has been studied using the geometric morphometrics methods proposed in the MORPHOJ 1.06d software (Klingenberg, 2011). As explained in Drake & Klingenberg (2010), shape variation was extracted from the coordinate data by a full Procrustes fit. To explore the intrafamilial differences and similarities of the bony labyrinth morphology, a principal component analysis (PCA) was performed. PCA geometric morphometrics results can be found in Supporting Information Data S1. A hierarchical analysis using the cluster analysis option of the PAST software (Ryan et al. 1995) has been performed. Considering that the coordinates of the semi-landmarks correspond to the general shape of the bony labyrinth, the analysis is based on all specimens PC scores (23 per specimen). Using the Euclidean similarity value option of PAST, the Euclidean distances can directly be assimilated to Procrustes distances.

Results

Anatomy and morphological variability of the bony labyrinth in *T. kanchil*

The bony labyrinth morphology of the fetus (NMB MAM 1532) and of the juvenile individuals is remarkably similar to that of the adults in size and in morphology. The overall volume of the bony labyrinth falls in the range of that of the adult specimens or is even a little bigger (Table 1). The cochlea shows some degree of variability in length (from

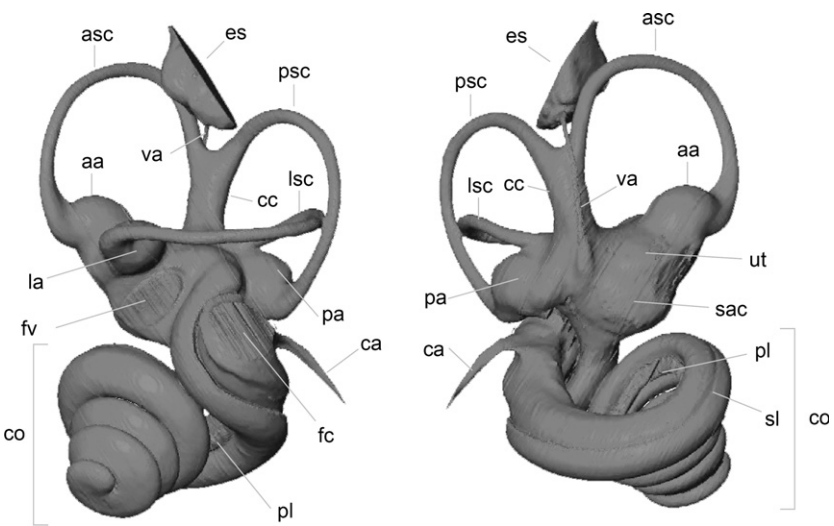

Fig. 1 Nomenclature used throughout the text illustrated on anteromedial and posterolateral views of *Tragulus kanchil* NMB C3797; aa, asc ampulla; asc, anterior semi-circular canal; ca, cochlear aqueduct; cc, common crus; co, cochlea; es, endolymphatic sac; fc, fenestra cochleae; fv, fenestra vestibuli; la, lsc ampulla; lsc, lateral semi-circular canal; pa, psc ampulla; pl, primary lamina; psc, posterior semi-circular canal; sac, saccule; sl, secondary lamina; ut, utricule; va, vestibular aqueduct.

Common crus:	1 landmark at the dorsal end
Anterior canal (9):	5 curves internal outline (1 for the ampulla)
	4 curves external outline
Posterior canal (9):	5 curves internal outline (1 for the ampulla)
	4 curves external outline
Lateral canal (10):	6 curves internal outline (1 for the ampulla)
	4 curves external outline
Stapedial fenestra (4):	4 curves each quarter
Cochlea (38):	3 curves thickness at ¼, ½ and ¾ of 1st turn
	3 curves thickness at ¼, ½ and ¾ of 2nd turn
	7 curves internal outline
	8 curves upper outline
	12 curves lateral outline
	11 curves lower outline
Vestibular aqueduct (1):	1 curve

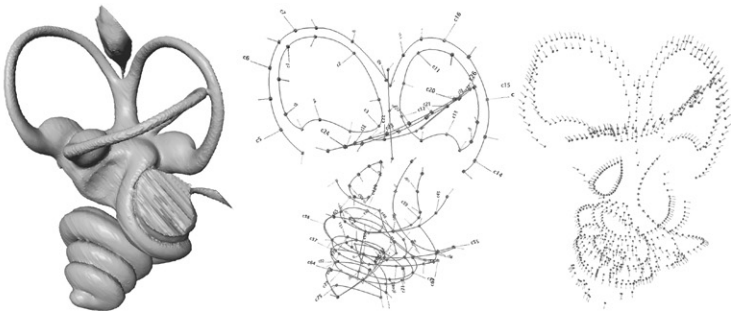

Fig. 2 Left bony labyrinth of *Tragulus kanchil* (NMBC3735) and list and location of the 77 curves and one landmark, representing 686 independent semi-landmarks used in this analysis.

34.77 to 39.15 mm in length) and number of turns (from 3.5 to 4 turns for the adults and from 3.5 to 3.75 turns for the juveniles, see Fig. 3 and Table 1). There is no significant correlation between the number of turns and length ($P > 0.1$), which means that the number of turns depends on the coiling pattern rather than on raw cochlear length. The cochlea is quite compact and high because of the large number of turns in comparison with other ruminants where it is known (Costeur, 2014). Aspect ratios (total height divided by total width) vary from 0.59 to 0.7. They classify *T. kanchil* in the high aspect ratios of Gray (1907) depicting high cochleas as opposed to flattened ones. The cochlear spiral is tight and only a maximum of half of the basal turn is detached from the rest of the cochlea (see Fig. 3). The last half of the basal turn can show slightly detached areas. The cochlear aqueduct, not ossified in the fetus NMB MAM 1532 (see Supporting Information Data S2), is invariably thin, flattened and bent towards the basal turn of the cochlea on the other specimens; it is not particularly long (Fig. 3). The secondary bony lamina is always present on the upper side of the curve of the basal turn, and it extends along its full length (Fig. 3). The fenestra cochleae is round to slightly oval in shape and faces laterally.

The vestibule has the same overall shape in all specimens. The stapedial ratio gives an idea of the elongation, or ellipsoid shape, of the fenestra ovale. It varies quite largely. Considering the adults, the values are between 1.65 and 1.9 with an average value at 1.75. The range is similar among the juveniles except for NMB C3806 and for the fetus NMB MAM 1532, where it is higher (Table 1), indicating a slightly more ellipsoid oval window, being pear-shaped in the fetus. Both the recessus sphaericus (corresponding to the sacculus) and the recessus ellipticus (corresponding to the utriculus) are well defined, with a sometimes fainter utriculus (NMB C3797 and NMB C3802). The saculus is slightly less developed on NMB C3795.

All three semi-circular canals taken separately are strikingly similar in size and shape. Only NMB C3802 has distinctly smaller anterior and posterior semi-circular canals. NMB MAM 1532 has relatively thinner middle parts of the canals due to small reconstruction problems related to an incomplete fully ossified and porous petrosal bone. The angles between the semi-circular canals in juveniles are in the same range as those measured for adult specimens, except for between the posterior and lateral semi-circular canals. The latter is slightly smaller than in adults (84.5–88° vs. 90–102°), but this is not the case in the fetus, where this angle was measured at 94°. The anterior semi-circular canal is the most expanded dorsally; it expands largely above the level of the common crus. The posterior semi-circular canal extends much less above the level of the common crus. The lateral semi-circular canal is slightly variable in shape. There is often a confluence with the posterior canal. It is sometimes very straight (e.g. NMB C.3735), sometimes a little more irregular (e.g. NMB C3791 and the juveniles), and even forms a strong wave in the fetus. There it meets the posterior semi-circular canal at a very high level. As a general rule, it branches dorsally to the posterior ampulla, in the vestibule between the posterior ampulla and the base of the common crus. Some variability in the branching position is observed where the lateral semi-circular canal is closer to the posterior ampulla. In dorsal or lateral view, the lateral canal extends beyond the plane of the posterior semi-circular canal. The three anterior, posterior and lateral ampullae are bulged in most of the adults and a little less in the juveniles and NMB C3802.

The common crus is slightly curved posterolaterally in all specimens. Its breadth and length are variable. The vestibular aqueduct and its overlying endolymphatic sac are similar in all *Tragulus* specimens. The aqueduct is a thin canal detached from the common crus over most of its course. It runs parallel to the midline of the common crus along its course, thus being also slightly curved posterolaterally, and extends slightly above the dorsal end of the common crus. Its curvature is variable. In NMB C3795, it is constant and follows the course of the common crus, whereas in NMB C3797, the aqueduct bends more sharply just above the level of the common crus. The endolymphatic sac ending the vestibular aqueduct is a pouch-like structure just above the common crus. It opens quickly outside the petrosal bone. However, it is very limited in the fetus NMB MAM 1532 due to the petrosal bone not being fully ossified in

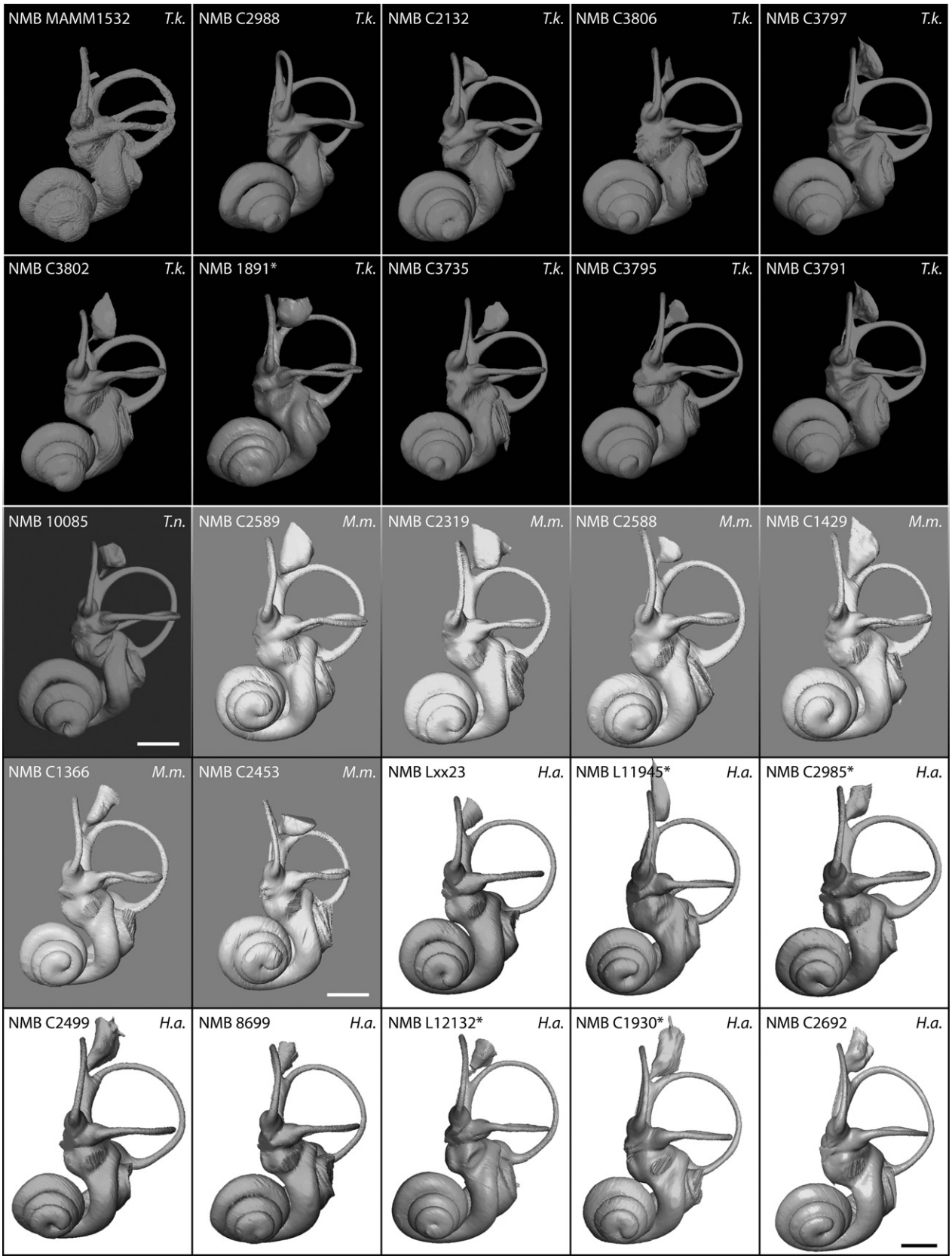

Fig. 3 Anterior view of the bony labyrinth of *Tragulus kanchil* (Black background, *T.k.*); *Tragulus napu* (dark grey background, *T.n.*); *Moschiola meminna* (light grey background, *M.m.*); *Hyemoschus aquaticus* (white background, *H.a.*). Scale bar: 2 mm.

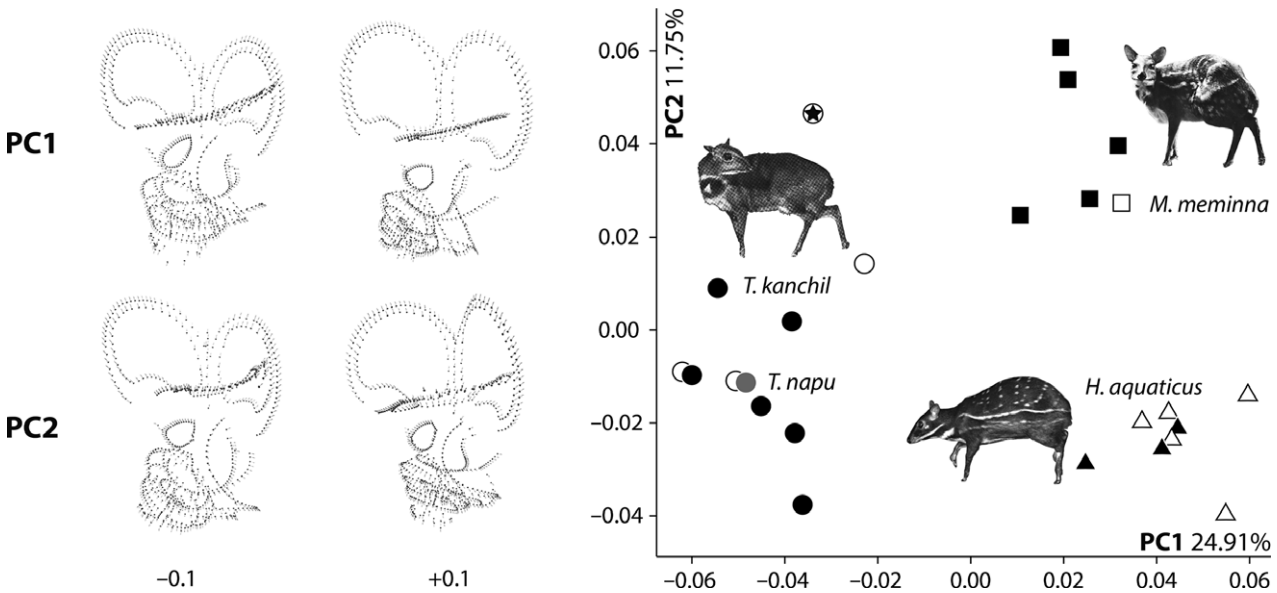

Fig. 4 Principal components analyses (PCA) based on the 3D coordinates of the tragulid bony labyrinth morphology. Circle: *Tragulus kanchil* (black); *Tragulus napu* (grey); Square: *Moschiola meminna*; Triangle: *Hyemoschus aquaticus*. The symbol with a star represents the fetus specimen, the empty symbols are the juveniles, and the filled symbols are the adults. PC shape variation is realized by the hypothetical bony labyrinth shapes at the extreme scores −0.1 and +0.1 on PC1 and PC2. Pictures of the three tragulids are from Nowak (1999).

this area. The slit-like opening is extremely angled so that the reconstructed pouch seems to be cut over its vertical extent. The shape of the sac contained within the petrosal bone is variable and as only the enclosed part of the sac was reconstructed, the latter slightly differs from one specimen to the other.

The bony labyrinth of *T. napu*

The bony labyrinth of *T. napu* NMB 10085 looks similar to that of *T. kanchil* (Fig. 3). No distinction based on geometric morphometrics analyses can be done (see below, and Fig. 4). However, some important characters are worth noting. The number of turns of the cochlea is slightly smaller, 3.25 turns. The total length of the cochlea is nonetheless in the same range, 37.66 mm (Table 1). This means the coiling pattern is less tightly coiled, which produces slightly longer turns in comparison with those of *T. kanchil*. The cochlear turns are more rounded than in *T. kanchil,* with a basal turn more detached from the vestibule than in *T. kanchil*. The secondary bony lamina sits high on top of the basal turn, whereas it is in a lower position in *T. kanchil*. The stapedial ratio (1.56) is smaller than in the T. *kanchil* sample, but we only have one specimen of *T. napu*, which does not account for species variability. While most of the semi-circular canal heights and widths are comparable, the height of the anterior semi-circular canal is larger than in *T. kanchil* (3.85 vs. an average of 3.52 with a maximum 3.75 in adult *T. kanchil*, but the oldest juvenile specimen NMB C3806 reaches 3.79, Table 1). There is no other particular difference in the shape of the semi-circular canals; the branching pattern of the lateral semi-circular canal is identical and the canal itself touches the posterior semi-circular canal as in several specimens of *T. kanchil*. The common crus in NMB 10085 is both longer and thinner than in *T. kanchil* (Fig. 3). The vestibular aqueduct and endolymphatic sac are similar to those of *T. kanchil*.

The bony labyrinth of *M. meminna* and *H. aquaticus*

Hyemoschus has a much bigger bony labyrinth, with a total volume of about 66 mm^3, almost twice the volume of *Tragulus* or *Moschiola*. The cochlea of both chevrotains is not as coiled as in *Tragulus*, with 2.75–3.5 and 2.75–3.25 turns in *Hyemoshus* and *Moschiola*, respectively. But the average cochlear aspect ratios (0.63 and 0.64, see Table 1) are comparable. The overall morphology of the whorls is similar to the condition observed in *Tragulus*. The cochlea of *Hyemoschus* is tightly coiled and very close to the vestibule, as in *Tragulus* but not in *Moschiola*, where it is a little more detached from the vestibule. The cochlear aqueduct is thinner in *Hyemoschus* and has a similar morphology in *Moschiola* and *Tragulus*.

The stapedial ratio of *Hyemoschus* (average 1.57, ovoid shape) is smaller than in *T. kanchil* (average 1.8 with juveniles included, ellipsoid shape) and even smaller in *Moschiola* (average 1.38, round shape).

Both chevrotains have a high branching pattern of the lateral semi-circular canal in the vestibule dorsal to the posterior ampulla such as in *Tragulus*. The lateral semi-circular canal is also slightly irregular, especially in *Moschiola*, and comes closer to (e.g. as in *Moschiola*) or touches (e.g. as in

Hyemoschus) the posterior semi-circular canal. Both conditions are observed in *Tragulus*. In dorsal or lateral view, the lateral canal extends beyond the plane of the posterior semi-circular canal as in *Tragulus*. The common crus is thin. The endolymphatic sac of *Moschiola* finishes the vestibular aqueduct over the common crus and is similar to that observed in *Tragulus*. It is more elongate and larger in *Hyemoschus* and does not cover the common crus as it does in the other tragulids.

3D Geometric morphometrics analyses of the Tragulidae bony labyrinths

The first axis (PC1) of the 23 PC score represents 24.91% of the total variance and the second one (PC2) 11.75% (see Data S1).

The shape changes observed along PC1 are the following (from negative to positive scores, see Fig. 4 and Data S1):

- the lateral canal is longer and wavy, touching the posterior canal, to shorter, well separated, and regular;
- the posterior semi-circular canal is shorter and ovoid, to longer and rounded;
- the anterior semi-circular is relatively square, to round;
- the anterior ampulla is bulged, to slightly flattened;
- the common crus is small and massive, to longer and thinner;
- the fenestra vestibuli is ellipsoid, to round;
- the sacculus is compressed, to wider;
- the vestibular aqueduct is central, to slightly anteriorly positioned;
- the origin of the cochlear aqueduct is low and close to the semi-circular canals, to high and more dorsally positioned;
- the first turn of the cochlea is directly perpendicular to the axis of the common crus, to slightly oblique to the latter;
- the first quarter of the cochlea is enlarged, to smaller;
- the cochlea is triangular in lateral shape, to rounder.

The shape changes observed along PC2 are the following (from negative to positive scores, see Fig. 4 and Data S1):

- the lateral semi-circular canal is regularly curved between the posterior and anterior semi-circular canals, to the lateral semi-circular canal is strongly bent on its posterior part;
- the lateral semi-circular canal has a regular thickness, to a proximal and distal enlarged end;
- the lateral semi-circular canal is elongated and straight, to shortened and wavy close to the posterior semi-circular canal;
- the posterior and anterior semi-circular canals have a similar height, to the anterior semi-circular canal is higher than the posterior one;
- the posterior semi-circular canal has a regular thickness, to a proximal and distal enlarged end;
- the vestibular aqueduct ends at the level of the common crus, to higher than the common crus;
- the vestibular aqueduct is bent, to straight along the common crus;
- the fenestra vestibuli is ovoid, to round;
- the second turn of the cochlea is close to the first turn, to slightly shifted at the level of the first quarter.

The distinction of the genera is only well supported by the association of the two first axes (see Data S1). No overlap between the three genera is observed (Fig. 4). The morphospace of *T. kanchil* observed on PC1 and PC2 is broader than that for *M. meminna* or *H. aquaticus* due to the position of the fetus NMB MAM 1532 on PC2. The morphospaces of *Moschiola* and *Hyemoschus* plot only on the positive scores of PC1, whereas *Tragulus* is concentrated exclusively in its negative scores (Fig. 4). The morphospace of *Moschiola* is separated from that of *Hyemoschus* based on PC2 scores (Fig. 4). All the *Moschiola* specimens plot in the positive domain of PC2, whereas *Hyemoschus* is restricted to the negative scores. *Tragulus* presents relatively low scores on PC2 (smaller than 0.2) except for the fetus NMB MAM 1532 (0.47, see Data S1). This can be explained by the fact that a small central part of the semi-circular canals (especially the lateral and posterior) is not fully ossified; thus, when reconstructing it, only the central part of the semi-circular canal was drawn. This explains why this specimen is attracted towards the high scores of PC2, considering that the proximal and distal ends of its canals are 'enlarged' (or in this case, the central part thinned down). Based on the semi-landmarks that we have defined, it is impossible to separate *T. kanchil* from *T. napu* (Fig. 4), *T. napu* being deeply nested within *T. kanchil*. No distinction between left bony labyrinths and reversed right ones can be observed.

The phenetic tree based on the general shape of the bony labyrinth (using the 23 PC coordinates) also shows that the three genera form three separated homogeneous morphospaces, respectively (Fig. 5). The entire *Tragulus* specimens form a cluster where *T. napu* is included, without any distinction to the other specimens. *Moschiola* and *Hyemoschus* form an unnatural cluster where *Moschiola* specimens are clearly separated from *Hyemoschus* (Fig. 5). The different ontogenetic stages are mixed with older specimens without any ordination or morphological trend (Figs 4 and 5). Looking at the phenetic tree, the fetus NMB MAM 1532 presents a general shape of the bony labyrinth very similar to that of the other *Tragulus* specimens (Fig. 5).

Comparison and discussion

Ontogeny of the bony labyrinth of *T. kanchil*

A fetal stage and three different post-natal ontogenetic stages in *T. kanchil* indicate that the bony labyrinth is

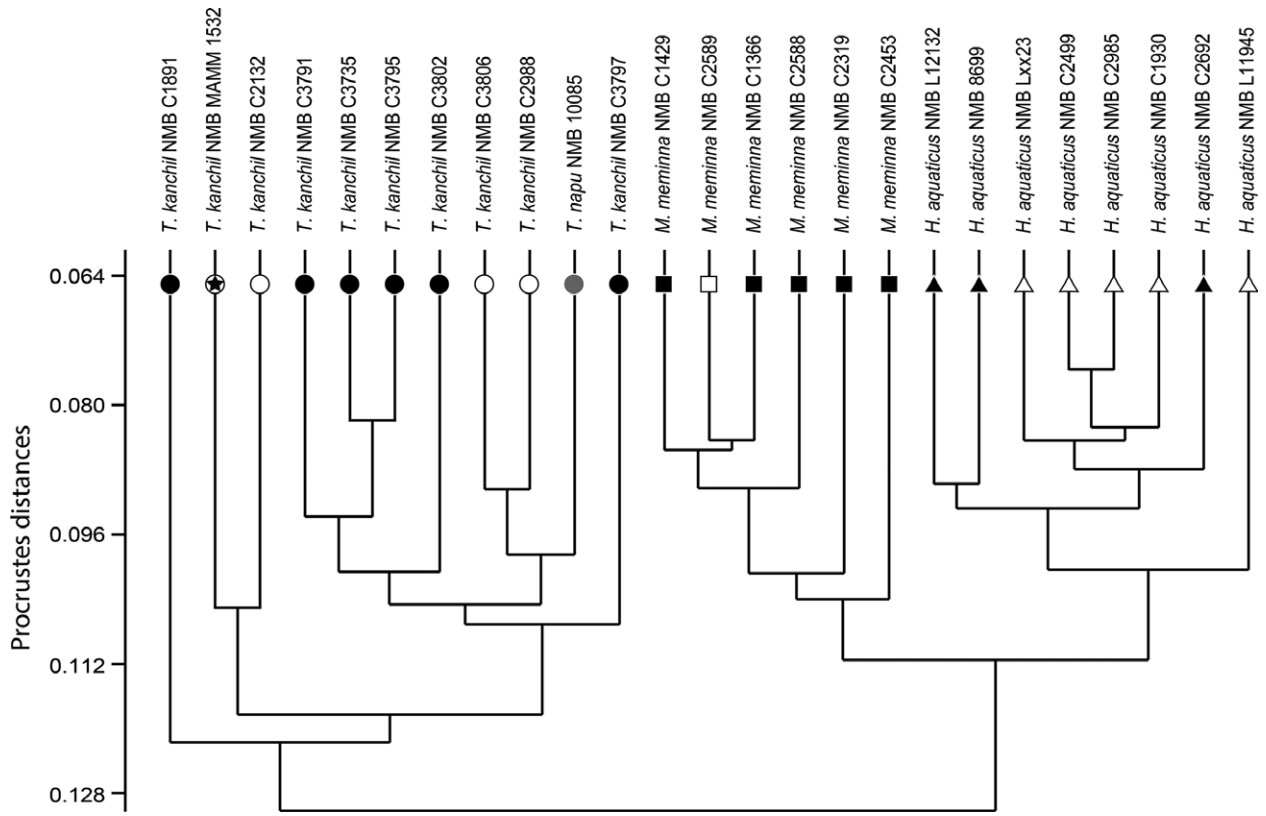

Fig. 5 Phenetic tree based on the Procrustes distances of the tragulid bony labyrinth landmark coordinates. The symbol legend is similar to those of Fig. 4.

almost fully formed even before birth (Figs 3 and 6). This confirms earlier observations (Maier, 2013) that ruminant petrosal bones containing the bony labyrinth are fully ossified around the time of birth. Our fetal individual shows that the petrosal bone is not yet fully ossified, being very porous, but the bony labyrinth is already essentially formed; only small parts of the posterior and lateral semi-circular canals, the endolymphatic sac and the cochlear aqueduct are missing (Figs 3 and 6). This is to be expected for ruminants, especially small animals, which need to be quickly fully functional to avoid predators. Young *Tragulus* individuals are reported to be fully formed and active at birth (Nowak, 1999). In addition, females of other *Tragulus* species (*T. javanicus* and *T. napu*) are known to be sexually mature at around 4.5–5 months of age, at about the same age as some rodents and much earlier than most other artiodactyls (Nowak, 1999; Dubost et al. 2010), confirming their early development. This is also confirmed by behavioural observations on *Hyemoschus* neonates and juveniles (Dubost, 1975). Nevertheless, open structures, i.e. the endolymphatic sac and the cochlear aqueduct, are not fully formed right before birth. In general, through ontogeny the shape of the lateral semi-circular canal is also variable (see Figs 3 and 6). This confirms variation of the planarity of the lateral semi-circular canal already evidenced in other mammals (Calabrese & Hullar, 2006; Ekdale, 2010). Much of the morphological variation observed on the four juvenile stages enters the natural morphological variation observed in adults, except maybe in the fetus, where the lateral semi-circular meets the posterior canal very dorsally (Figs 3 and 6).

Previous studies mostly carried out on marsupials (*Didelphis*: Larsell et al. 1935; *Monodelphis*: Ekdale, 2010; *Calauromys*: Sánchez-Villagra & Schmelzle, 2007) show that the petrosal bone and the bony labyrinth in the investigated taxa are not yet ossified at birth. The bony labyrinth looks fully functional but is still membranous. The cochlea is also shorter at birth and grows by up to more than 1.5 turns in *Didelphis* (Larsell et al. 1935). In other mammals where ontogenetic change of the bony labyrinth has been investigated, such as in *Macaca mulatta* (Daniel et al. 1982), morphological change is likely to occur but size does not change, confirming our observations. The changes are associated to rotation of the cochlea after birth in *Macaca*. No such change has been evidenced here, even when a fetal stage is considered. Extensive changes observed in the bony labyrinth of marsupials are correlated to reproduction strategy where the baby is not autonomous after birth. In *Macaca*, parent care still persists after birth, whereas in *Tragulus* it only continues for a very short time (Nowak, 1999).

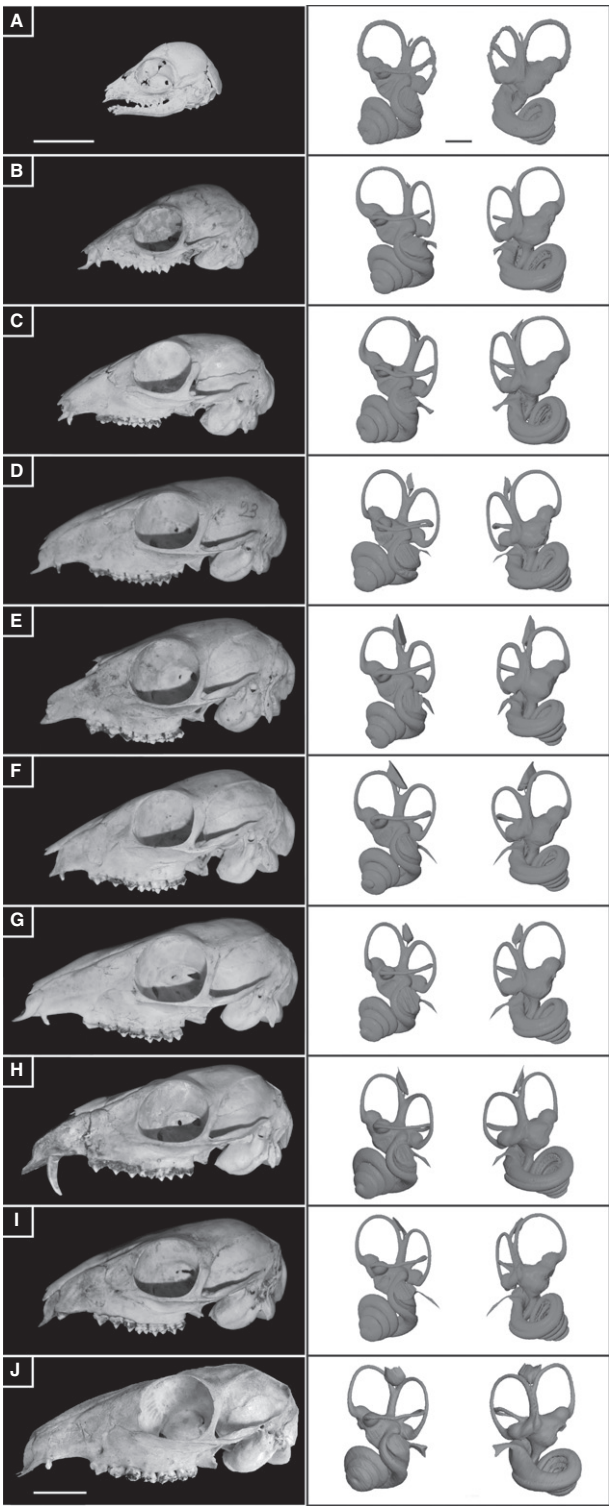

Fig. 6 Ontogenetic series of *Tragulus kanchil* scanned for this study and their reconstructed bony labyrinth in lateral and cerebellar views, respectively. A, 3D reconstruction of a fetus (NMB MAMM 1532). B-D, three juvenile stages (NMB C2988, NMB C2132, and NMB C3806), E-I, six adults stages (NMN C3802, NMB C3797, NMB C3735; NMB C3791, NMB C3795, NMB C1891). Scale bar: 2 cm (skulls); 2 mm (bony labyrinth).

The bony labyrinths in our fetal and juvenile specimens are not smaller than those of the adults; indeed, their total volume and size are similar (Fig. 6, Table 1). The total volume of the bony labyrinth is even slightly larger in the fetus and the juvenile specimens than in the adults. This could indicate that while compacting and ossifying completely during growth, the voids in which the membranous labyrinth is contained tend to shrink slightly. Our study confirms that the bony labyrinth does not grow after birth in ruminants. This first described artiodactyl fetal bony labyrinth represents a third of total braincase height and we show that it does not grow larger during ontogeny (Fig. 6). Negative allometry of the bony labyrinth within the petrosal has been evidenced in placental mammals (Billet et al. 2015), albeit never on an ontogenetic series. The petrosal bone has to grow through the life of an individual to be able to stay in contact with the surrounding skull (Koyabu et al. 2014), but petrosal size remains relatively small even in large mammals (Billet et al. 2015; L. Costeur, pers. obs.). Within an ontogenetic trajectory such as that studied here in *T. kanchil*, the bony labyrinth does not grow through the life of an individual, but the skull more than doubles in length. The size of the petrosal bone was not measured in our sample but it is expected to grow slightly through the animal's life to keep in contact with the growing skull. This was also observed on petrosal bones of *Giraffa camelopardalis* (a juvenile NMB 2197 and an adult NMB 12075) where the juvenile petrosal bone is smaller and less massive than the adult one (Schmutz, 2014). Billet et al. (2015) indicated that mostly the outgrowth of the petrosal bone would be likely to expand (e.g. epitympanic wing, medial flange of the promontorium). This was also described for baleen whales (Bisconti, 2001). Our observations confirm this hypothesis already evidenced in marsupials (Ekdale, 2010). The petrosal bone of the fetus is a mere container for the bony labyrinth, where the latter is only covered by a thin bony cover.

Intraspecific morphological variability

Variation linked to the laterality is not higher than the intraspecific variability. The shape and length of the common crus is variable within the three investigated genera. The number of turns of the cochlea varies by a maximum of half a turn or by 13% in total length (Table 1). It falls within the 'most coiled' cochleas as far as mammals are concerned (Ekdale, 2010). Such a variability in cochlear length is known in humans and longer cochleas seem to indicate higher sensory capacities in given areas of the cochlea because of a higher number of sensory cells (Úlehlová et al. 1987; Ericson et al. 2009). Variability of the cochlea in *T. kanchil* was thus not unexpected and it means that different individuals of the same species of ruminants can also show different hearing capacities, as the size of the cochlea has been shown to be strongly correlated to the range of hearing frequencies

(Kirk & Gosselin-Ildari, 2009). To the best of our knowledge, this has never been shown for ruminants. However, it is not likely to represent a very large difference in hearing capacities. Indeed cochlear size does not seem to play such a great role in lower frequency hearing limit and it is rather the ratio between the basal and the apical turns that is important (Manoussaki et al. 2008). The overall volume of the bony labyrinth varies by $< 15\%$ in adults (from 31.8 to 38.8 mm^3, Table 1) and seems to be in agreement with variability observed in primates (Gunz et al. 2012).

Mammals with very specific behaviours such as the three-toed sloth *Bradypus* (slow motion behaviour) show a large morphological variability in the shape of the lateral semi-circular canal (Billet et al. 2012). As the semi-circular canals are associated to balance and locomotion, strong constraints can be expected to explain their shape, as well as the angles between them. Billet et al. (2012) indicated that a release of constraints in *Bradypus* may explain why the lateral canal is so variable in shape. In accordance with other cursorial or fast-moving mammals and although the shape of the lateral semi-circular canal varies, *T. kanchil* does not show this amount of variation observed in *Bradypus*. *Tragulus kanchil* is a cursorial small artiodactyl living in densely forested environments where fast-moving behaviours are important as hiding strategies to avoid predators (Rössner, 2007). The angles between the semi-circular canals vary by a maximum of 17.5° in our study of *T. kanchil* or 18.4° in *M. meminna* (Table 1) within the range of the 20° evidenced in domestic horses (Danilo et al. 2015).

Phylogenetic interest of intrageneric and intrafamilial variability and stability of the bony labyrinth

The comparison of the *T. kanchil* sample with both *T. napu* and to the other living tragulid genera *Hyemoschus* and *Moschiola* confirmed that the bony labyrinth is at least genus-specific in tragulids, as it is in other mammals (Spoor & Zonneveld, 1995; Gunz et al. 2012; Ekdale, 2013; Macrini et al. 2013; Billet et al. 2015; Mennecart & Costeur, in press; Figs 4 and 5). We suspect similar results within all the Ruminantia. The reconstruction of the bony labyrinth of *T. napu* shows several important differences captured by discrete characters rather than by the overall 3D shape. As such, it provides relevant information for phylogenetic reconstructions. The range of morphological variation within a species such as *T. kanchil* does not prevent it from being differentiated from another closely related species. Inside the same genus, the shape and size of the common crus may well represent an interesting character despite some variation observed within *T. kanchil*; the common crus is thinner and longer in *T. napu*. The cochlear coil also seems to be different, being smaller in *T. napu* than in *T. kanchil*, although total cochlear length is identical (Table 1). The same is true for the stapedial ratio is concerned, which is smaller in *T. napu* (Fig. 3, Table 1). A PCA based on classical morphometric data (graph not shown here, data from Table 1) reveals that 75% of the total variance (PC1) is explained by size (volume of the bony labyrinth and centroid size) allowing a distinction between *Hyemoschus* and the other genera. The PC2 (10% of the total variance) separates *Tragulus* from *Moschiola* based on the angle between the lateral and posterior semi-circular canals. Geometric morphometrics analyses allow a much more precise distinction based on morphology.

Some characters and character states are shared by the three studied genera, such as the insertion of the lateral semi-circular canal dorsal to the posterior ampulla and in the vestibule (Mennecart & Costeur, in press; Fig. 3). Likewise, the expansion of the lateral semi-circular canal beyond the plane of the posterior semi-circular canal in dorsal or lateral view is typical of tragulids within ruminants (Mennecart & Costeur, in press). This condition of the lateral canal occurs neither in the family Moschidae (extant and extinct; see Costeur, 2014) nor in a published limited sample of Bovidae and Cervidae (Costeur, 2014; Costeur et al. 2014).

The morphological variability of the bony labyrinth and the ossification timing of the petrosal suggested by the late fetal stage, may be of phylogenetic interest. The open structures (cochlear aqueduct, endolymphatic sac) are not present in the youngest specimen, whereas the semi-circular canals are almost fully formed and the cochlea is complete.

The endolymphatic sac is variable in size and shape within Tragulidae. This structure is similar in closely related taxa, as in the sister genera *Tragulus* and *Moschiola*, with a pinched sac overhanging the common crus (Fig. 3). A recent phylogenetic analysis (Mennecart & Costeur, in press) considers it as a synapomorphy of this clade. This does not confirm previous observations (Billet et al. 2015) made on xenarthrans and rhinocerotids, where the length of the vestibular aqueduct seems to be correlated with body size rather than with taxonomic affinities. This does not appear to be the case in ruminants (observations made on the minute species *Oreotragus oreotragus*, Klipspringer NMB 8401, and on the very large species *G. camelopardalis*, Giraffe NMB 12075). Moreover, the shape of the cochlear aqueduct is variable within our *T. kanchil* sample but it is very similar to those observed in the closely related *Moschiola*. Billet et al. (2015) showed how allometric this structure could be in some placentals, confirming an earlier study (Ekdale, 2010). Great care has to be taken when using the cochlear aqueduct in phylogenetic analyses, especially considering its absence in our fetal specimen.

The lateral semi-circular canal is almost fully ossified in the fetus. Spoor et al. (2007), among others, link the morphology of this structure to the locomotory abilities of the animals. However, it has been recently demonstrated that this variable structure is also highly informative to differentiate ruminants with similar ecology and locomotion at the

family level (see Costeur, 2014; Costeur et al. 2014; Mennecart & Costeur, in press).

The different lengths and shapes of the cochlea between the three tragulid genera probably indicates different hearing capacities. No study has ever investigated the hearing capacities in Tragulids. To what extent these differences could be used for phylogenetic analyses is still poorly known (see discussion in Ekdale, 2010) as great variation in cochlear length and morphology is known across clades. Nevertheless, the same number of turns of the cochlea known in adults is already present on the fetus specimen in an almost fully ossified petrosal bone. This number of turns straightforwardly distinguishes the Tragulidae from the pecoran ruminants (Mennecart & Costeur, in press). We expect this condition to appear early in the evolutionary history of ruminants. Mennecart & Costeur (in press) confirmed this hypothesis in a Middle Miocene Tragulidae showing a typical tragulid number of cochlear turns.

In addition, the stapedial ratio is shown here to be highly variable within a species, from 1.65 to 1.9 in our adult sample and up to 1.98 when juveniles are considered. Average values in both *Hyemoschus* and *Moschiola* are very different and would show some phylogenetic relevance (*contra* Ekdale, 2010). Similarly, a list of characters that are likely to be of little use in phylogenetic analyses in horses and their relatives has been proposed (Danilo et al. 2015); we confirm that some of these characters are variable, such as the length of the common crus. However, our comparison of *T. kanchil* and *T. napu* seems to indicate that its shape may be of interest.

Conclusions

This is the first study investigating the ontogeny and morphological variability in the ruminant bony labyrinth. We confirm that the bony labyrinth does not grow after birth in ruminants. Although the petrosal bone is still porous in a late fetal stage, the bony labyrinth itself is almost fully formed (size and shape) before birth, except for some open structures (endolymphatic sac and cochlear aqueduct). The petrosal bone is fully ossified in an early post-natal stage, confirming that full ossification occurs before birth or around the time of birth. It grows only slightly during the lifetime in ruminants, and only in places independent of the bony labyrinth itself. The bony labyrinth thus reaches adult size and is fully functional very early in the life of *Tragulus*. This finding is in accordance with observations made on tragulids in the wild, where young animals are very quickly independent from their mother. Using a 3D Geometric morphometrics analysis, we observe that the range of morphological variability in juvenile stages is not greater than that evidenced in a set of adult specimens, except for the late fetal stage. The planarity of the lateral semi-circular canal may not yet be completely acquired in juveniles, but this character is known to be variable in other mammals. The length of the cochlea can vary by a half a turn and its length by a little more than 10%. The length and shape of the common crus is variable, too, with thin and elongate common crus or short and more massive ones. The angles between the canals also vary and show a range of variation known in other placentals. This study shows the morphologically quite conservative nature of the ruminant bony labyrinth and its specificity at the species level. Ontogenetic changes are small. They mostly entail the natural variability observed in an adult sample. Contrary to other parts of the skeleton, the use of isolated petrosals for bony labyrinth reconstructions where the age of the individual is impossible to estimate, thus represents no major problem and is encouraged.

Comparison with another species of the same genus shows strong similarity but also exploitable differences, such as a different common crus (shape) or cochlea (number of turns and shape). Our study shows how different the bony labyrinth of sister taxa within a ruminant family can be and validates its use for taxonomic or phylogenetic studies; it confirms the potential evidenced in other mammal groups. Timing of ossification of the petrosal bone and acquisition of bony labyrinth structures bring a lot of information concerning phylogeny. Thus, the open structures that appear later in the ontogeny (endolymphatic sac and cochlear aqueduct) are very similar in closely related genera. The semi-circular canals, which ossify earlier, allow families to be distinguished. The cochlea, which ossifies very early, may help to make distinctions at the infra-order level within the Ruminantia (i.e. Tragulina vs. Pecora).

Acknowledgements

Georg Schulz and Bert Müller (Biomaterial Science Center, University of Basel) are thanked for greatly helping with CT-scans. We are grateful to Urs Wuesst (Naturhistorisches Museum Basel) for helping us in finding the *Tragulus* fetus. Special thanks go to Tandra Fairbanks Freund (USA citizen, NMB) who greatly improved the English quality of the article.

Basil Thüring (Naturhistorisches Museum Basel, Department of Geosciences) is warmly thanked for continuous support in this long-lasting project on ruminant inner ears. The Stiftung zur Förderung des NMB and the Kugler-Werdenberg Stiftung are thanked for financial support. The Swiss National Foundation is warmly thanked for granting the SNF Project 200021_159854/1. We thank Anthony Graham, Maeva Orliac, and Eric G. Ekdale for their constructive comments, which helped improve this paper.

Authors' contributions

B.M. and L.C. designed the study, scanned the skulls, segmented the bony labyrinths, performed the analyses, and wrote the paper together. L.C. described the bony labyrinths. B.M. performed the geometric morphometrics analyses.

References

Alloing-Séguier L, Sánchez-Villagra MR, Lee MSY, et al. (2013) The bony labyrinth in diprotodontian marsupial mammals: diversity in extant and extinct forms and relationships with size and phylogeny. *J Mamm Evol* **20**, 191–198.

Benoit J, Lehmann T, Vatter M, et al. (2015) Comparative anatomy and three-dimensional geometric morphometric study of the bony labyrinth of Bibymalagasia (Mammalia, Afrotheria). *J Vert Paleontol* **35**, e930043.

Billet G, Hautier L, Asher RJ, et al. (2012) High morphological variation of vestibular system accompanies slow and infrequent locomotion in three-toed sloths. *Proc R Soc B* **279**, 3932–3939.

Billet G, Hautier L, Lebrun R (2015) Morphological diversity of the bony labyrinth (inner ear) in extant xenarthrans and its relation to phylogeny. *J Mammal* **96**, 658–672.

Bisconti M (2001) Morphology and postnatal trajectory of rorqual petrosal. *Ital J Zool* **68**, 87–93.

Calabrese DR, Hullar TE (2006) Planar relationships of the semicircular canals in two strains of mice. *J Assoc Res Otolaryngol* **7**, 151–159.

Costeur L (2014) The petrosal bone and inner ear of *Micromeryx flourensianus* (Artiodactyla, Moschidae) and inferred potential for ruminant phylogenetics. *Zitteliana B* **32**, 1–16.

Costeur L, Schulz G, Müller B (2014) High-resolution X-ray computed tomography to understand ruminant phylogeny. *Proc SPIE* **9212**, 921216–1–921216–7.

von Cramon-Taubadel N, Frazier BC, Mirazón Lahr M (2007) The problem of assessing landmark error in geometric morphometrics: theory, methods, and modifications. *Am J Phys Anthropol* **134**, 24–35.

Daniel HJ, Schmidt RT, Olshan AF, et al. (1982) Ontogenetic changes in the bony labyrinth of *Macaca mulatta*. *Folia Primatol* **38**, 122–129.

Danilo L, Rémy J, Vianey-Liaud M, et al. (2015) Intraspecific variation of endocranial structures in extant *Equus*: a prelude to endocranial studies in fossil equoids. *J Mamm Evol* **22**, 561–582.

David R, Droulez J, Allain R, et al. (2010) Motion from the past. A new method to infer capacities of extinct species. *C R Palevol* **9**, 397–410.

Davies KT, Bates PJ, Maryanto I, et al. (2013) The evolution of bat vestibular systems in the face of potential antagonistic selection pressures for flight and echolocation. *PLoS ONE* **8**, e61998.

Drake AG, Klingenberg CP (2010) Large-scale diversification of skull shape in domestic dogs: disparity and modularity. *Amer Nat* **175**, 289–301.

Dubost G (1975) Le comportement du Chevrotain africain, Hyemoschus aquaticus Ogilby (Artiodactyla, Ruminantia). Sa signification écologique et phylogénétique. *Z Tierpsychol* **37**, 449–501.

Dubost G, Charron F, Courcoul A, et al. (2010) The Chinese water deer, *Hydropotes inermis* – a fast-growing and productive ruminant. *Mamm Biol* **76**, 190–195.

Ekdale EG (2010) Ontogenetic variation in the bony labyrinth of *Monodelphis domestica* (Mammalia: Marsupialia) following ossification of the inner ear cavities. *Anat Rec* **293**, 1896–1912.

Ekdale EG (2013) Comparative anatomy of the bony labyrinth (inner ear) of placental mammals. *PLoS ONE* **8**, e66624.

Ericson E, Högstorp H, Wadin K, et al. (2009) Variational anatomy of the human cochlea: implications for cochlear implantation. *Otol Neurotol* **30**, 14–22.

Gentry A, Rössner GE, Heizmann EPJ (1999) Suborder Ruminantia. In: *The Miocene Land Mammals of Europe* (edsRössner GE, Heissig K), pp. 225–258. Munich: Verlag Dr. Friedrich Pfeil.

Geraads D (2010) Tragulidae. In: *Cenozoic Mammals of Africa* (edsWerdelin L, Sanders W), pp. 723–729. Los Angeles: University of California Press.

Gray AA (1907) *The Labyrinth of Animals: Including Mammals, Birds, Reptiles and Amphibians*, vol. **1**. London: J and A Churchill.

Gray AA (1908) *The Labyrinth of Animals: Including Mammals, Birds, Reptiles and Amphibians*, vol. **2**. London: J and A Churchill.

Grohe C, Tseng ZJ, Lebrun R, et al. (2015) Bony labyrinth shape variation in extant Carnivora: a case study of Musteloidea. *J Anat*. doi:10.1111/joa.12421.

Groves C, Grubb P (2011) *Ungulate Taxonomy*. Baltimore: The Johns Hopkins University Press.

Gunz P, Ramsier M, Kuhrig M, et al. (2012) The mammalian bony labyrinth reconsidered, introducing a comprehensive geometric morphometric approach. *J Anat* **220**, 529–543.

Hassanin A, Delsuc F, Ropiquet A, et al. (2012) Pattern and timing of diversification of Cetartiodactyla (Mammalia, Laurasiatheria), as revealed by a comprehensive analysis of mitochondrial genomes. *C R Biologies* **335**, 32–50.

Hillson S (1986) *Teeth*. Cambridge: Cambridge University Press.

Hyrtl J (1845) *Verleichende-anatomische Untersuchungen über das innere Gehörorgan des Menschen und der Säugethiere*. Prague: Verlag von Friedrich Ehrlich.

Jeffery N, Spoor F (2004) Prenatal growth and development of the modern human labyrinth. *J Anat* **204**, 71–92.

Kirk EC, Gosselin-Ildari AD (2009) Cochlear labyrinth volume and hearing abilities in primates. *Anat Rec* **292**, 765–776.

Klingenberg CP (2011) MorphoJ: an integrated software package for geometric morphometrics. *Mol Ecol Resour* **11**, 353–357.

Koyabu D, Werneburg I, Morimoto N, et al. (2014) Mammalian skull heterochrony reveals modular evolution and a link between cranial development and brain size. *Nat Commun* **5**,. doi:10.1038/ncomms4625.

Larsell O, McCrady E Jr, Zimmermann AA (1935) Morphological and functional development of the membranous labyrinth in the opossum. *J Comp Neurol* **63**, 95–118.

Lebrun R, Ponce de León MS, Tafforeau P, et al. (2010) Deep evolutionary roots of strepsirrhine primate labyrinthine morphology. *J Anat* **216**, 368–380.

Macrini TE, Flynn JJ, Ni X, et al. (2013) Comparative study of notoungulate (Placentalia, Mammalia) bony labyrinths and new phylogenetically informative inner ear characters. *J Anat* **223**, 442–461.

Maier W (2013) The entotympanic in late fetal Artiodactyla (Mammalia). *J Morphol* **275**, 926–939.

Manoussaki D, Chadwick RS, Ketten DR, et al. (2008) The influence of cochlear shape on low-frequency hearing. *Proc Natl Acad Sci U S A* **105**, 6162–6166.

Meijaard E, Groves C (2004) A taxonomic revision of the *Tragulus* mouse-deer (Artiodactyla). *Zool J Linn Soc* **140**, 63–102.

Mennecart B, Costeur L (in press) A *Dorcatherium* (Mammalia, Ruminantia, Middle Miocene) petrosal bone and the tragulid ear region. *J Vert Paleontol*.

Mennecart B, Métais G (2015) *Mosaicomeryx* gen. nov., a ruminant mammal from the Oligocene of Europe and the significance of 'gelocids'. *J Sys Palaeontol* **13**, 581–600.

Mennecart B, Becker D, Berger J-P (2011) *Iberomeryx minor* (Mammalia, Artiodactyla) from the Early Oligocene of Soulce (Canton Jura, NW Switzerland): systematics and palaeodiet. *Swiss J Geosci* **104**(suppl. 1), S115–S132.

Métais G, Chaimanee Y, Jaeger J-J, et al. (2001) New remains of primitive ruminants from Thailand: evidence of the early evolution of the Ruminantia in Asia. *Zool Scr* **30**, 231–248.

Nowak RM (1999) *Walker's Mammals of the World*, 6th edn, vol. **2**. Baltimore: The Johns Hopkins University Press.

Orliac M, Benoit J, O'Leary MA (2012) The inner ear of *Diacodexis*, the oldest artiodactyl mammal. *J Anat* **221**, 417–426.

Pfaff C, Martin T, Ruf I (2015) Bony labyrinth morphometry indicates locomotor adaptations in the squirrel related clade (Rodentia, Mammalia). *Proc R Soc B* **282**, 20150744.

Rössner G (2007) Tragulidae. In: *The Evolution of Artiodactyls* (eds Prothero DR, Foss SE), pp. 213–220. Baltimore: The Johns Hopkins University Press.

Ryan PD, Harper DAT, Whalley JS (1995) *PALSTAT, Statistics for Palaeontologists*. Chapman & Hall (now Kluwer Academic Publishers). Downloadable on http://folk.uio.no/ohammer/past/ (consulted in 2015).

Sánchez IM, Quiralte V, Rios M, et al. (2014) First African record of the Miocene Asian mouse-deer *Siamotragulus* (Mammalia, Ruminantia, Tragulidae): implications for the phylogeny and evolutionary history of the advanced selenodont tragulids. *J Sys Paleontol* **13**, 543–556.

Sánchez-Villagra MR, Schmelzle T (2007) Anatomy and development of the bony inner ear in the wooly opossum, *Caluromys philander* (Didelphimorphia, Marsupiala). *Mastozool Neotrop* **14**, 53–60.

Schmelzle T, Sánchez-Villagra MR, Maier W (2007) Vestibular labyrinth diversity in diprotodontian maruspial mammals. *Mamm Study* **32**, 83–97.

Schmutz SB (2014) *Is Palaeomeryx (Mammalia, Ruminantia) a Sister Taxon to the Giraffidae? Insights from the Petrosal Bone and Inner Ear*. Unpublished Master Thesis. Basel: Geologisch-Paläontologisches Institut der Universität Basel, 160 p.

Schwarz C (2012) *Phylogenetische und funktionsmorphologische Untersuchungen der Ohrregion bei Sciuromorpha (Rodentia, Mammalia)*. Unpublished Ph.D. Thesis. Bonn: Rheinischen Friedrich-Wilhelms-Universität, 350 p.

Solntseva GN (2010) Morphology of the inner ear of mammals in ontogeny. *Russ J Dev Biol* **41**, 94–110.

Spoor F, Zonneveld FW (1995) Morphometry of the primate bony labyrinth: a new method based on high-resolution computed tomography. *J Anat* **186**, 271–286.

Spoor F, Zonneveld F (1998) Comparative review of the human bony labyrinth. *Am J Phys Antrhopol* **107**, 211–251.

Spoor F, Garland T, Krovitz G, et al. (2007) The primate semicircular canal system and locomotion. *Proc Natl Acad Sci U S A* **104**, 10808–10812.

Toyoda S, Shiraki N, Yamada S, et al. (2015) Morphogenesis of the inner ear at different stages of normal human development. *Anat Rec* **298**, 2081–2090.

Úlehlová L, Voldřich L, Janisch R (1987) Correlative study of sensory cell density and cochlear length in humans. *Hear Res* **28**, 149–151.

Van Arsdel WC III, Hilleman HH (1951) The ossification of the middle and internal ear of the golden hamster (*Cricetus auratus*). *Anat Rec* **109**, 673–689.

Wiley D (2006) *Landmark Editor 3.6. Institute for Data Analysis and Visualization. Davis: University of California*. Downloadable on http://graphics.idav.ucdavis.edu/research/EvoMorph (consulted in 2015).

Wilson DE, Reeder DM (2005) *Mammal Species of the World*. Baltimore: The Johns Hopkins University Press.

Supporting Information

Additional Supporting Information may be found in the online version of this article:

Data S1. Geometric morphometrics dataset containing: the average shape coordinates, the principal component eigenvalues and variance, the Procrustes coordinates of the specimens, and the coordinates of the hypothetical shape at the PC1 and PC2 values −0.1 and +0.1.

Data S2. Bony labyrinth of a fetus of *Tragulus kanchil* (NMB MAMM 1532).